Dalton Transactions

Accepted Manuscript

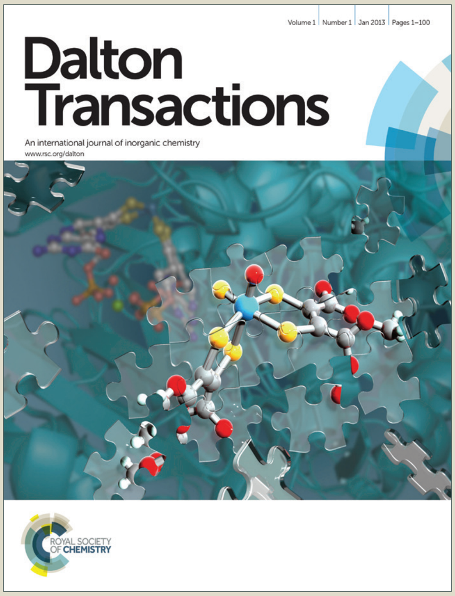

ROYAL SOCIETY OF CHEMISTRY

www.rsc.org/dalton

Journal Name

RSCPublishing

ARTICLE

Tetraphenolate niobium and tantalum complexes for the ring opening polymerization of ε-caprolactone

Cite this: DOI: 10.1039/x0xx00000x

Received 00th January 2012,
Accepted 00th January 2012

DOI: 10.1039/x0xx00000x

www.rsc.org/

Yahya Al-Khafaji,[a] Xinsen Sun,[a] Timothy. J. Prior,[a] Mark R.J. Elsegood,[b] and Carl Redshaw,[a*]

Abstract: Reaction of the pro-ligand α,α,α′,α′-tetra(3,5-di-*tert*-butyl-2-hydroxyphenyl–*p*-)xylene-*para*-tetraphenol (p-L^1H_4) with two equivalents of $[NbCl_5]$ in refluxing toluene afforded, after work-up, the complex $\{[NbCl_3(NCMe)]_2(\mu\text{-}p\text{-}L^1)\}\cdot6MeCN$ (**1**·6MeCN). When the reaction was conducted in the presence of excess ethanol, the orange complex $\{[NbCl_2(OEt)(NCMe)]_2(\mu\text{-}p\text{-}L^1)\}\cdot3\frac{1}{2}MeCN\cdot0.614$toluene (**2**·3½MeCN·0.614toluene) was formed. A similar reaction using $[TaCl_5]$ afforded the yellow complex $\{[TaCl_2(OEt)(NCMe)]_2(\mu\text{-}p\text{-}L^1)\}\cdot5MeCN$ (**3**·5MeCN). In the case of the *meta* pro-ligand, namely α,α,α′,α′tetra(3,5-di-*tert*-butyl-2-hydroxyphenyl–*m*-)xylene-*meta*-tetraphenol (m-L^2H_4) only the use of $[Nb(O)Cl_3(NCMe)_3]$ led to the isolation of crystalline material, namely the orange bis-chelate complex $\{[Nb(NCMe)Cl(m\text{-}L^2H_2)_2]\}\cdot3\frac{1}{2}MeCN$ (**4**·3½MeCN) or $\{[Nb(NCMe)Cl(m\text{-}L^2H_2)_2]\}\cdot5MeCN$ (**4**·5MeCN). The molecular structures of **1** – **4** and the tetraphenols L^1H_4 and m-$L^2H_4\cdot2MeCN$ have been determined. Complexes **1** – **4** have been screened as pre-catalysts for the ring opening polymerization of ε-caprolactone, both with and without benzyl alcohol or solvent present, and at various temperatures; conversion rates were mostly excellent (> 96 %) with good control either at > 100 °C over 20 h (in toluene) or 1 h (neat).

Keywords: Niobium; tantalum; tetraphenolate; crystal structure; ε-caprolactone; ring opening polymerization

Introduction

The ring opening polymerization (ROP) of lactides and lactones continues to attract interest as a source of biodegradable polymeric materials.[1] Whilst some metals (and non-metals) have been employed in a variety of catalysts for such ROP processes, the use of other metals such as niobium and tantalum has received scant attention. Indeed, only two reports, namely on systems using a tripodal trialkoxyamine ligand with $Ta(OEt)_5$[2] and more recently the use of bi-dentate phenoxyimines in combination with $NbCl_5$[3] have been reported for the ROP of either lactides or lactones. These metals are also now attracting interest for α-olefin polymerization catalysis.[4] Given the lack of use of these group V metals, we have initiated a program to explore their potential for ROP using a variety of ancillary ligands at the metal. We noted with interest the new family of tetraphenols recently reported by Wasserman *et al.*[5], and also that they have since been exploited by the group of Wu to prepare multi-alkali metal complexes capable of the ROP of *L*-lactide.[6] Herein, we explore the coordination chemistry of these tetraphenols towards niobium and tantalum, and investigate the capability of the resulting complexes (see scheme 1) towards the ROP of ε-caprolactone under a variety of conditions.

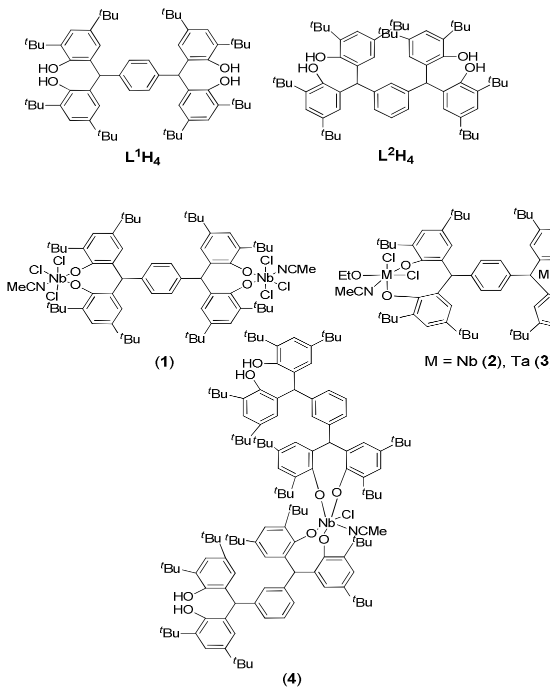

Scheme 1

---

[a] *Department of Chemistry, University of Hull, Hull, HU6 7RX, U.K.*
[b] *Chemistry Department, Loughborough University, Loughborough, Leicestershire, LE11 3TU, U.K.*

The nature of the products has allowed us to also screen for possible cooperative effects. We have noted for organoaluminium-based ROP systems, that the presence of nearby metal centres can either be beneficial or detrimental depending on the separation distance and type of bonding present,[7] whilst others have noted large effects in olefin polymerization.[8]

Results and Discussion

Synthesis and structure of p-L^1H_4 derived niobium and tantalum complexes

The ligand L^1H_4 was synthesized following the reported literature method.[5] It proved possible to grow small single crystals, which were suitable for X-ray diffraction using synchrotron radiation. The molecular structure is shown in Figure 1, with crystallographic data presented in Table 3. There are two half molecules on centres of symmetry in the asymmetric unit; there is no solvent of crystallization. Within both unique molecules, there are strong C–H···π interactions between one of the unique hydroxyl groups and the central C_6 ring: H(1)···C(16) = 2.18 Å, angle at H(1) = 144°; H(3A)···C(48) = 2.26 Å, angle at H(1) = 142°. There are also weaker C–H···π interactions between the other hydroxyl group and a phenolic ring: H(2)···C(6) = 2.43 Å, angle at H(1) = 139°; H(4)···C(38) = 2.38 Å, angle at H(1) = 142°. In the packing of the molecules, there are weak O–H···O intermolecular interactions at *ca.* 2.43 Å between H(2) and O(4$^{/}$) and H(4) and O(2$^{/}$) with angles of *ca.* 109°, but the lengths are very long and the angle sub-optimal for these interactions to be significant.

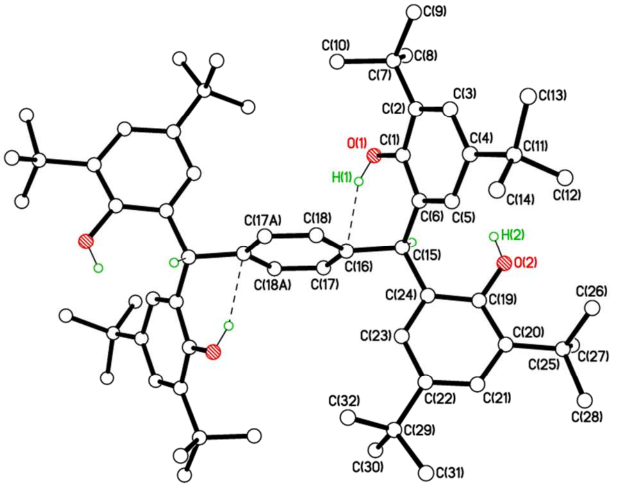

Figure 1. Molecular structure of L^1H_4, indicating the atom numbering scheme. Non-OH hydrogen atoms have been removed for clarity. The second unique molecule is not shown but has similar geometry.

The compound $\{[NbCl_3(NCMe)]_2(\mu\text{-}p\text{-}L^1)\}$MeCN (**1**·6MeCN) was synthesized in good yield (*ca.* 83 %) via the treatment of L^1H_4 with a slight excess (2.1 equiv.) of $[NbCl_5]$ in refluxing toluene. The reaction proceeds with loss of two equivalents of HCl per metal centre. In the IR spectrum of **1**, *v*(CN) for the coordinated acetonitrile is observed at 2308/2286 cm^{-1}. The ^{1}H NMR signals/integrals are consistent with the formulation for **1** (see experimental section). Crystals suitable for a single crystal X-ray diffraction study were grown from a saturated acetonitrile solution at 0 °C; the crystal structure is presented in Figure 2. Each niobium centre is present in a distorted octahedral geometry, and bears a *mer* arrangement of chlorides with the sixth position *trans* to one of the phenoxide groups occupied by an acetonitrile molecule. The two sets of diphenolates across the central phenyl ring are arranged in a *trans* fashion related by an inversion centre. The bond lengths and angles are given in the caption to Figure 2; the Nb – O distances [1.860(5) and 1.879(5) Å] are typical of those observed in previous niobium(V) aryloxides,[9] with the shortest value found *trans* to the acetonitrile ligand. The Nb – Cl distances [*ca*. 2.38 Å] are slightly longer than those observed in $[Nb_2Cl_{10}]$ [2.250(6) and 2.302(5) Å] and $[NbCl(mtp)_2]$ [2.3357(9) Å] ($mtpH_2$ = 2,2$^{/}$-methylene-bis(2,4-di-*tert*-butylphenol), but shorter than observed in $[Nb(NCMe)Cl(ebp)_2]$ [2.4339(10) Å] ($ebpH_2$ = 2,2$^{/}$-ethylidene-bis(2,4-di-*tert*-butylphenol).[10] The Nb – N distance of 2.270(6) is comparable with that of $[NbCl_5(NCMe)]$ [2.236(4) Å],[11] and the binding is linear [Nb(1) – N(1) – C(33) 170.3(6)°]. An 8-membered metallocycle is formed at each end of the tetraphenolate, with each adopting the boat conformation; the bite angle of the chelate is 96.6(2)°.

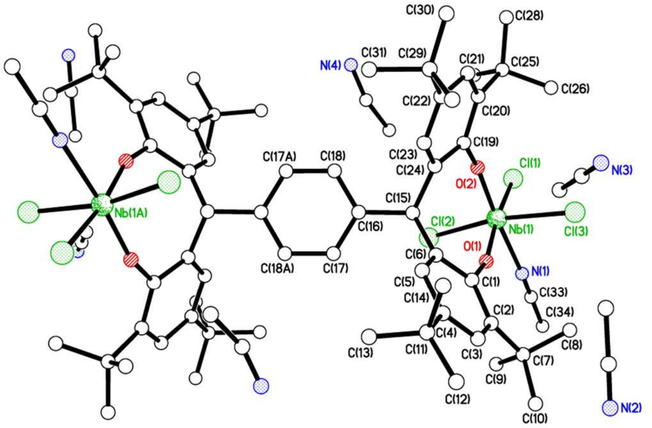

Figure 2. Representation of the molecular structure of complex **1**·6MeCN in the solid state, indicating the atom numbering scheme. Hydrogen atoms have been removed for clarity. Selected bond lengths (Å) and angles (°): Nb(1) – O(1) 1.879(5), Nb(1) – O(2) 1.860(5), Nb(1) – Cl(1) 2.380(2), Nb(1) – Cl(2) 2.3860(19), Nb(1) – Cl(3) 2.3828(19), Nb(1) – N(1) 2.270(6); O(1) – Nb(1) – O(2) 96.6(2), Nb(1) – O(1) – C(1) 159.5(4), Nb(1) – O(2) – C(19) 153.8(4), O(1) – Nb(1) – Cl(1) 170.45(14).

If the above reaction was conducted in the presence of excess ethanol, then a complex of formula $\{[NbCl_2(OEt)(NCMe)]_2(\mu\text{-}p\text{-}L^1)\}$·3½MeCN·0.614toluene (**2**·3½MeCN·0.614toluene) was isolated in good yield. In the IR spectrum of **2**, *v*(CN) for the coordinated acetonitrile is observed at 2312/2290 cm^{-1}. The ^{1}H NMR signals/integrals are consistent with the formulation for **2** (see experimental section). Crystals suitable for a single crystal X-ray diffraction study were grown from a saturated acetonitrile solution at 0 °C; the crystal structure is presented in Figure 3. Interestingly, the molecule has two distinct ends and two distinct faces. At one end, Nb(1) has ethoxide and acetonitrile *trans*, with both chlorides *trans* to phenolates. At the other end, Nb(2) has ethoxide *trans* to one chloride, whilst the two phenolates are *trans* to a chloride and acetonitrile.

Furthermore, one face of the tetraphenolate supports both metal centres, whilst the other face has none. Thus, an acetonitrile lies below the central C_6H_4 ring at the Nb(1) end, while a chloride lies below the ring at the Nb(2) end; this contrasts with the centro-symmetric arrangement found in **1**. Spectroscopically, the non-symmetrical nature of **2** probably accounts for the multiple *v*CN stretches noted in the IR spectrum. Molecules of **2** pack in layers giving zones with hetero atoms (Cl, N, O) and zones with hydrocarbon moieties (^{t}Bu groups and toluene molecules). There are a few weak, intermolecular C–H···Cl/O/N interactions.

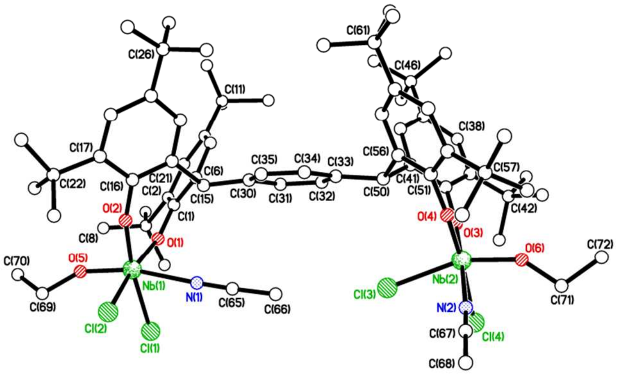

Figure 3. Representation of the molecular structure of complex **2**·3½MeCN·0.614toluene in the solid state, indicating the atom numbering scheme. Hydrogen atoms, and unbound solvent molecules have been removed for clarity. Selected bond lengths (Å) and angles (°): Nb(1) – O(1) 1.897(2), Nb(1) – O(2) 1.915(2), Nb(1) – O(5) 1.826(2), Nb(1) – Cl(1) 2.4116(10), Nb(1) – Cl(2) 2.3964(10), Nb(1) – N(1) 2.300(3); O(1) – Nb(1) – O(2) 89.72(9), Nb(1) – O(1) – C(1) 154.1(2), Nb(1) – O(2) – C(16) 159.75(19), Nb(1) – O(5) – C(65) 148.9(3).

Similar use of [$TaCl_5$] led to the isolation of the complex {[$TaCl_2(OEt)(NCMe)]_2$(μ-*p*-L^1)}·5MeCN (**3**·5MeCN) in good yield. Crystals suitable for a single crystal X-ray diffraction study were grown from a saturated acetonitrile solution at 0 °C; the crystal structure is presented in Figure 4. The unit cells of **2**·3½MeCN and **3**·5MeCN are very similar as are the molecular structures. The tetraphenoxide ligand acts as a bidentate ligand to two pairs of Ta(V) cations; O(1) and O(2) are deprotonated and bind in a *cis* chelating fashion to Ta(1). The coordination is completed by a pair of *cis* chloride ligands, one ethoxide, and one molecule of acetonitrile. Ta(2) is bound by O(3) and O(4) and has very similar coordination. The ligands on the two Ta(V) ions are arranged such that the acetonitrile bound to Ta(2) is oriented towards Cl(2) along the long axis of the complex, a situation reminiscent of **2**; as for 2, there are multiple *v*CN stretches in the IR spectrum observed at 2334/2318/2290 cm^{-1} . Adjacent complexes are packed such that there are weak C–H···Cl interactions between bound acetonitrile of one molecule and chloride ions in the next. These assemble the complexes into stacks running parallel to the crystallographic *a* axis. Unbound, but crystallographically well-determined, acetonitrile also forms weak C–H···Cl interactions. A portion of diffuse electron density was modelled using the SQUEEZE routine, in particular that centred on 0, ½, ½ in the unit cell. This suggested the presence of approximately two further molecules of acetonitrile per unit cell and a composition of [{$TaCl_2(MeCN)(C_2H_5O)$}$_2$(tetraphen)]·4MeCN.

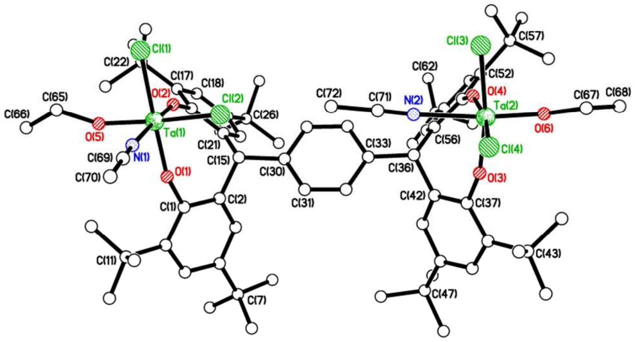

Figure 4. Representation of the molecular structure of complex **3**·5MeCN in the solid state, indicating the atom numbering scheme. Hydrogen atoms, and unbound solvent molecules have been removed for clarity. Selected bond lengths (Å) and angles (°):Ta(1) – O(1) 1.883(9), Ta(1) – O(2) 1.866(8), Ta(1) – O(5) 1.842(8), Ta(1) – Cl(1) 2.431(3), Ta(1) – Cl(2) 2.437(3), Ta(1) – N(1) 2.275(11); O(1) – Ta(1) – O(2) 92.5(3), Ta(1) – O(1) – C(1) 155.2(7), Ta(1) – O(2) – C(16) 155.9(8), Ta(1) – O(5) – C(65) 144.9(10).

Synthesis and structure of m-L^2H_4 derived niobium

The ligand L^2H_4 was synthesized following the reported literature method.[5] It proved possible to grow small single crystals from a saturated acetonitrile solution. Although the diffraction data was weak, the connectivity is clear. The molecular structure is shown in Figure 5, with crystallographic data presented in Table 2. There are two acetonitrile molecules of crystallization, both of which are H-bonded to an OH group. There is also an intramolecular O–H···π interaction: O(2)–H(2)···C(30) = 2.31 Å, akin to those seen in L^1H_4. Molecules form centrosymmetric pairs encapsulating pairs of symmetry-related acetonitrile molecules (see ESI, Figure S1). Otherwise there are only van der Waal's forces between molecules.

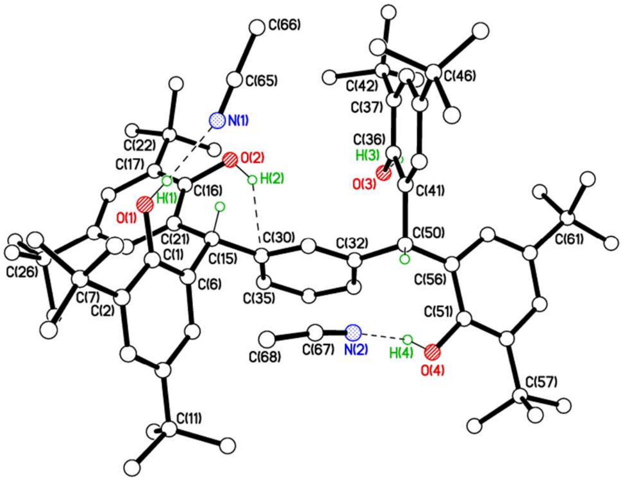

Figure 5. Molecular structure of L^2H_4·2MeCN, indicating the atom numbering scheme. Non-OH hydrogen atoms have been removed for clarity.

Similar treatment (as for L^1H_4) of the *meta* ligand L^2H_4 with a slight excess of [$NbCl_5$] (or $TaCl_5$) failed to afford any crystalline material. Instead, we found that only use of the oxychloride complex [$NbOCl_3(NCMe)_2$] allowed access to clean products. Reaction of [$NbOCl_3(NCMe)_2$)] (two equivalents) with L^2H_4 afforded, following work-up, an orange solid **4**. In the IR spectrum of **4**, *v*(CN) for the coordinated acetonitrile is observed at 2295/2261 cm^{-1}, whilst bands at 3545/3523/3428 cm^{-1} were assigned to *v*(OH). However, the structure of **4** was not obvious from the ^1H NMR signals/integrals. Single crystals were obtained from a saturated acetonitrile on prolonged standing at ambient temperature. The structure was found to comprise two L^2H_2 ligands per Nb centre, namely {[Nb(NCMe)Cl(*m*-L^2H_2)$_2$]}·3½MeCN (**4**·3½MeCN). Given the unexpected nature of this product, the reaction was repeated to verify reproducibility, and again single crystals were obtained from saturated acetonitrile solutions following work-up of the interaction of [$NbOCl_3(NCMe)_2$] (two equivalents) and L^2H_4. The product on this again proved to differ only in the degree of solvation, *viz* {[Nb(NCMe)Cl(*m*-L^2H_2)$_2$]}·5MeCN (**4**·5MeCN). The molecular structure of **4**·3½MeCN is shown in Figure 5, with selected bond lengths and angles given in Table 1 (and compared with those of **4**·5MeCN); a diagram of **4**·5MeCN is given in the ESI, Figure S2.

Table 1. Selected structural data for **4**·3½MeCN and **4**·5MeCN

Bond lengths (Å)/Angles (°)	**4**·3½MeCN	**6**·5MeCN
Nb1−O1	1.886(3)	1.873(7)
Nb1−O2	1.933(3)	1.925(8)
Nb1−O5	1.921(3)	1.928(8)
Nb1−O6	1.946(3)	1.916(8)
O1−Nb1−O2	92.95(12)	93.8(3)
O2−Nb1−O5	174.37(13)	173.0(3)
Nb1−O1−C1	157.4(3)	156.6(8)
Nb1−O2−C16	154.1(3)	155.1(7)
Nb1−O5−C65	160.7(3)	158.2(9)

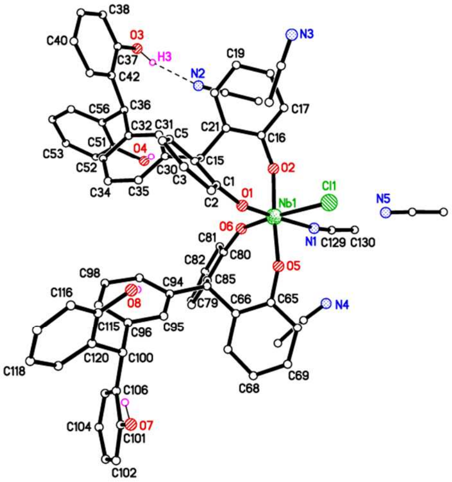

Figure 6. Molecular structure of **4**·3½MeCN. Hydrogen atoms except O*H*, and tBu groups have been removed for clarity.

In the asymmetric unit, the formula is 2[NbCl(NCMe)(meta-L^2H_2)$_2$]·5MeCN. The Nb(V) is octahedral, bonding to one chloride ligand, one acetonitrile, and two chelating meta-L^2H_2 ligands. The Cl^- and NCMe are *cis*. Two diphenol-diphenolates bind through proximal phenolates and form a pair of 8-membered chelate rings. The phenols at the opposite end of each *meta*-L^2H_2 ligand are not deprotonated. One of the O(8) atoms forms a hydrogen bond to a molecule of MeCN. Further acetonitrile of solvation is included in the structure. For each Nb, 4.5 molecules of MeCN are modelled as point atoms. A further portion of diffuse electron density corresponding to 0.5MeCN was modelled using the SQUEEZE procedure. There are weak inter- and intra-molecular C–H···Cl interactions within the solid that knit together pairs of complexes into dimers held by Nb−Cl···H−C interaction. Otherwise, the packing is unremarkable.

The crystal of **4**·5MeCN examined was very weakly scattering. Diffraction data did not extend beyond $2\theta = 40$ ° (Mo radiation, $\lambda = 0.71073$ Å). Despite the poor scattering, a good solution was obtained. This gives very useful chemical information: the metal coordination is essentially the same as in **4**·3½MeCN. The major difference is the degree of solvation which gives rise to a different packing arrangement.

Polymerization Screening

Compounds **1** - **4** were screened for the ring opening polymerization of ε-caprolactone (ε-Cl). Each catalyst has been screened for polymerization with and without addition of BnOH (benzyl alcohol) and at different temperatures, times and Nb:ε-Cl ratios. From the screening (Table 2), it is evident that activity was only observed at temperatures in excess of 100 ^oC; recently reported niobium phenoxyimines were also found to operate at high temperatures.[3] Comparing complexes **1** and **2** suggests that, in toluene, the presence of the ethoxides in **2** is beneficial in terms of conversion and control (runs 1 – 4 *versus* 6 – 10), whilst both systems appear to perform better in the absence of solvent (runs 5 and 11), though there was a slight increase in control. With or without toluene present, the niobium ethoxide **2** afforded a bimodal distribution of products (see ESI, Figure S3), whereas the isostructural tantalum complex **3** afforded only a lower molecular weight fraction. Based on entries 11 to 15, there is a near linear relationship between monomer conversion and number average molecular weight (M_n) for the lower molecular weight fraction, with narrow molecular distributions (≤1.26); similar plots for the high molecular weight fraction are also near linear with PDI≤1.9 (see ESI, Figures S4 and S5). Moreover, plots (see ESI, Figures S6 and S7) of M_n (low or high molecular weight fraction) *versus* [CL]/[**2**] had a near linear relationship, suggestive of a living system. Increasing the molar ratio of ε-Cl:Nb (for 2) from 200:1 to 800:1 led to an increase in the observed molecular weights (of both fractions) with the conversion rates and molecular weight distributions remaining relatively constant for the lower fraction (1.14 – 1.26), whilst as the ratio increased the spread of molecular weights for the higher fraction decreased; increasing the ratio beyond 800:1 had no further effect.

The results using complex **4** in toluene suggested that the presence of just one niobium centre can be beneficial in terms of conversion, for example runs 4 v 27, however when an ethoxide is present at niobium, then the system performs better in terms of conversion, control and increased molecular weight (runs 12 v 27). Interestingly, in the absence of benzyl alcohol, complex 4 was the only system involving niobium to afford PCL (run 26). When the ROP was conducted the absence of solvent, **4** exhibited inferior conversion (50 %) *versus* **1** and **2** (98 %), but better control (runs 6 and 16 *versus* 28).

In the MALDI-TOF spectra (see ESI, Figures S8), only one major population of peaks, possessing the spacing of 114 mass unit (the molecular weight of the monomer), was detected. The peaks are assigned to the sodium adducts of the polymer chains with benzyloxy end groups. A smaller series of peaks is associated with the use of protonated/sodiated (from the matrix) species from the matrix.[12]

The ^{1}H NMR spectrum of the polymer was obtained (for an example see ESI, Figure S9) to verify the molecular weight of the polymer and identify the end chain group of the PCL (polycaprolactone). Typically, peaks at δ 7.38, 5.07 and 3.65 ppm (5:2:2) indicated that the polymer chains were capped by one benzyl ester and a hydroxyl group, consistent with insertion of a benzyloxy group during polymerization.

Run	**Cat.**	**Toluene**	**CL:X[b]:BnOH**	**T/ °C**	**t/h**	**m/g**	**Conversion (%)**	**M_nx10^{-4}[c]**	**PDI[c]**
1	1	5	400:1:2	25	1	---	---	---	---
2	1	5	400:1:2	80	1	---	---	---	---
3	1	5	400:1:0	100	20	---	---	---	---
4	1	5	400:1:2	110	1	0.03	50	0.12	**1.07**
5	1	5	400:1:2	110	20	0.10	86	0.66	**1.25**
6	1	---	200:1:0.5	100	1	4.65	98	0.18	**1.77**
7	2	5	400:1:2	25	1	---	---	---	---
8	2	5	400:1:2	80	1	---	---	---	---

Table 2 Ring opening polymerization of ε-CL using **1-4**[a]

9	2	5	400:1:2	110	1	---	---	---	---
10	2	5	400:1:0	110	20	---	---	---	---
11	2	5	200:1:2	110	20	0.03	96	0.70 (6.66)	**1.18** **(1.9)**
12	2	5	400:1:2	110	20	0.39	99	0.94 (7.31)	**1.14** **(1.67)**
13	2	5	600:1:2	110	20	0.17	98	1.09 (8.97)	**1.12** **(1.58)**
14	2	5	800:1:2	110	20	0.49	97	1.18 (11.44)	**1.26** **(1.44)**
15	2	5	1000:1:2	110	20	0.42	97	1.19 (12.13)	**1.26** **(1.4)**
16	2	---	200:1:0.5	100	1	2.1	98	0.24 (7.34)	**1.31** **(1.80)**
17	3	5	400:1:2	25	1	---	---	---	---
18	3	5	400:1:2	80	1	---	---	---	---
19	3	5	400:1:2	110	1	---	---	---	---
20	3	5	400:1:0	110	20	0.31	98	0.21	**1.73**
21	3	5	400:1:2	110	20	0.20	98	0.26	**1.20**
22	3	---	200:1:0.5	100	1	1.69	98	0.31	**1.20**
23	4	5	400:1:2	25	1	---	---	---	---
24	4	5	400:1:2	80	1	---	---	---	---
25	4	5	400:1:2	110	1	---	---	---	---
26	4	5	400:1:0	110	20	0.02	96	0.11	**1.11**
27	4	5	400:1:2	110	20	0.24	98	0.24	**1.31**
28	4	---	200:1:0.5	100	1	2.81	50	0.36	**1.17**

[a] Conditions: 12.3 µmol of cat.; 1.0 M ε-CL toluene solution. [b] X= Nb,Ta complexes. [c] GPC data in THF *vs.* polystyrene standards.

In summary, a number of new tetraphenolate niobium (and tantalum) complexes have been prepared from the metal precursors [MCl_5] (M= Nb, Ta) or [$NbOCl_3(NCMe)_2$]. Crystal structure determinations reveal a preference for binding two metal centres when using then ‘*para*’ ligand set L^1H_4, whereas use of the ‘*meta*’ ligand L^2H_4 resulted in the isolation of a bis(chelate) mononuclear complex. In terms of the ROP of ε-caprolactone, only negligible polymer was isolated at temperatures below 100 °C. At 100 °C, in the absence of any solvent, these systems were capable of good conversions (≥98 %) in the case of the dinuclear systems; 50 % conversion was observed for the mononuclear system. In toluene, the presence of an ethoxide at the metal was generally advantageous in terms of conversion and control.

Experimental

General

All manipulations were carried out under an atmosphere of dry nitrogen using conventional Schlenk and cannula techniques or in a conventional nitrogen-filled glove box. Diethyl ether and tetrahydrofuran were refluxed over sodium and benzophenone. Toluene was refluxed over sodium. Dichloromethane and acetonitrile were refluxed over calcium hydride. All solvents were distilled and degassed prior to use. IR spectra (nujol mulls, KBr or NaCl windows) were recorded on a Nicolet Avatar 360 FT IR spectrometer; ^1H NMR spectra were recorded at room temperature on a Varian VXR 400 S spectrometer at 400 MHz or a Gemini 300 NMR spectrometer or a Bruker Advance DPX-300 spectrometer at 300 MHz. The ^1H NMR spectra were calibrated against the residual protio impurity of the deuterated solvent. Elemental analyses were performed by the elemental analysis service at the London Metropolitan University. The ligands L^1H_4 and L^2H_4 were prepared as described in the literature.[5] The precursor [$Nb(O)Cl_3(NCMe)_2$] was prepared via $(Me_3Si)_2O$.[13]

Synthesis of {[$NbCl_3(NCMe)]_2(\mu$-*p*-L^1)}·6MeCN (**1**·6MeCN)

α,α,α′,α′-Tetrakis(3,5-di-*tert*-butyl-2-hydroxyphenyl)-*p*-xylene L^1H_4 (1.66 g, 1.80 mmol) was dissolved in toluene (40 mL). $NbCl_5$ (1.00 g, 3.70 mmol) was added as a solid and the system was refluxed for 12 h. The volatiles were removed *in vacuo,* and the residue was extracted into warm acetonitrile (30 ml); prolonged standing at 0 °C gave orange plates of the compound **1** (2.46 g, 83 %). MS (positive nanospray in CH_2Cl_2/MeCN): 1364.5 (M – Cl), 1323.5 (M – Cl – MeCN), 1211.6 (M – 3Cl – 2MeCN), 1176.2 (M – 3Cl – 2MeCN). Found: C, 59.06; H, 6.63; N 0.77. $C_{68}H_{92}Cl_6N_2O_4Nb_2$ (sample dried *in vacuo* for 12 h; -7MeCN) requires C, 58.33; H, 6.60; N, 1.03 %. IR (Nujol, KBr, cm^{-1}): 2308w, 2286w, 1645w, 1568w, 1303w, 1235m, 1171bs, 1118s, 1087m, 1019w, 1009w, 904m, 886s, 829m, 815s, 721s, 639w, 559m, 545m, 479w, 446w. ^1H NMR

(Acetoned$_6$): δ = 7.20 – 6.78 (overlapping m, 12H, aryl*H*), 6.07 (2H, C*H*), 2.05 (s, 6H, *Me*CN), 1.38 (s, 36H, C(CH_3)$_3$), 1.15 (s, 36H, C(CH_3)$_3$).

{[NbCl$_2$(OEt)(NCMe)]$_2$(μ-*p*-L^1)}·3½MeCN·0.614toluene (**2**·3½MeCN·0.614toluene)

To NbCl$_5$ (0.59 g, 2.18 mmol) in toluene (20 ml) at -78 °C was added ethanol (5 ml) and the solution was stirred for 5 min., following which L^{1}H$_4$ (1.00 g, 1.08 mmol) in toluene(10 ml) was added and the mixture was then stirred for 48 h at ambient temperature. After the volatiles were removed *in-vacuo*, the residue was extracted into acetonitrile (20 ml) or dichloromethane (20 ml) and on prolonged standing (1 – 2 days) at ambient temperature, red prisms of **2** formed (1.84 g, 63 %). MS MS (positive nanospray in CH$_2$Cl$_2$/MeCN): 1333 (M – EtOH – MeCN). IR (Nujol, KBr, cm^{-1}): 2313w, 2290w, 1626w, 1598w, 1570w, 1506w, 1405m, 1362s, 1292m, 1256m, 1230s, 1198s, 1154m, 1104s, 1094s, 1054s, 1020s, 974w, 916s, 880s, 862s, 816w, 799m, 776m, 761m, 659m, 645w, 615w, 594w, 556m, 464m, 453m. Found: C, 57.55;* despite repeated attempts, samples gave unsatisfactory C values; H, 7.58; N, 0.59. C$_{70}$H$_{99}$Cl$_4$O6NNb$_2$ (sample dried *in vacuo* for 12 h; -4.5MeCN – 0.614toluene) requires C, 61.00; H, 7.24; N, 1.02 %. ^{1}H NMR (CDCl$_3$): δ = 7.31 – 7.15 (overlapping m, 15H, aryl*H* + 0.614C$_6H_5$CH$_3$), 5.04 (bm, 4H, OCH_2 + C*H*), 4.15 (bm, 2H, OCH_2), 2.33 (0.614C$_6$H$_5$CH_3), 1.98 (bs, 10.5H, 3.5*Me*CN), 1.45 (s, 36H, C(CH_3)$_3$), 1.22 (s, 36H, C(CH_3)$_3$), 1.20 (m, 3H, OCH$_2$CH_3), 1.15 (m, 3H, OCH$_2$CH_3).

{[TaCl$_2$(OEt)(NCMe)]$_2$(μ-*p*-L^1)}·5MeCN (**3**·5MeCN)

As for **2**, but using TaCl$_5$ (0.78 g, 2.18 mmol) and L^{1}H$_4$ (1.00 g, 1.08 mmol) affording **3** as yellow crystals (1.38 g, 75 %). Found: C, 55.06; H, 7.03; N, 0.34. C$_{72}$H$_{102}$Cl$_4$N$_2$O$_4$Ta$_2$ (sample dried *in vacuo* for 12 h; -6.5MeCN) requires C, 54.03; H, 6.41; N, 0.46 %. IR (Nujol, KBr, cm^{-1}): 2334w, 2318w, 2290w, 1676w, 1573w, 1296s, 1256s, 1238s, 1154s, 1111s, 1073s, 1020s, 971w, 917w, 889m, 810w, 761s, 721s, 658w, 582w, 553m, 444w. MS (solvated with CH$_2$Cl$_2$ and diluted with MeCN for positive nano-electrospray technique): *m/z* 1404 [MH – 3Cl – OEt – MeCN)]$^+$. ^{1}H NMR (Acetoned$_6$): δ = 7.26 – 6.74 (overlapping m, 12H, aryl*H*), 6.07 (m, 2H, C*H*), 3.54 (m, 4H, OCH_2), 1.30 (s, 36H, C(CH_3)$_3$), 1.22 (m, 3H, OCH$_2$CH_3), 1.15 (s, 36H, C(CH_3)$_3$), 1.11 (m, 3H, OCH$_2$CH_3). *Me*CN obscured by solvent.

Synthesis of L^{2}H$_4$·2MeCN

L^{2}H$_4$ (1.00 g) was dissolved in MeCN (20 ml). On prolonged standing (2 days) small off-white prisms of L^{2}H$_4$·2MeCN formed. Yield: 0.88 g, 81 %. Found: C, 81.12; H, 9.69; N, 2.81. C$_{64}$H$_{90}$O$_4$·2MeCN requires C, 81.22; H, 9.62; N, 2.79 %. IR (Nujol, KBr, cm^{-1}): 3555m, 3524m, 3430m, 2296w, 2261w, 1782w, 1601w, 1584w, 1416m, 1388m, 1377s, 1317w, 1292m, 1261m, 1209m, 1190s, 1153m, 1122m, 1084m, 1022m, 987w, 970w, 928w, 912w, 813m, 770w, 760w, 719w, 669w, 645w, 604w, 562w, 508w, 467w, 445w. ^{1}H NMR (CDCl$_3$): δ = 6.59 – 7.29 (4x m, 12H, aryl*H*), (5.54 (s, 2H, C*H*), 4.71 (s, 4H, O*H*), 1.99 (bs, 6H, 3.5*Me*CN), 1.35 (s, 36H, C(CH_3)$_3$), 1.14 (s, 36H, C(CH_3)$_3$).

Synthesis of {[Nb(NCMe)Cl(*m*-L^{2}H$_2$)$_2$]}·3½MeCN (**4**·3½MeCN) and {[Nb(NCMe)Cl(*m*-L^{2}H$_2$)$_2$]}·5MeCN (**4**·5MeCN).

α,α,α′,α′-Tetrakis(3,5-di-*tert*-butyl-2-hydroxyphenyl)-*m*-xylene (L^{2}H$_4$, 4.10 g, 4.44 mmol) and [Nb(O)Cl$_3$(NCMe)$_3$] (2.61 g, 8.78 mmol) were refluxed in toluene (40 ml) for 12 h. On cooling, volatiles were removed *in-vacuo*, and the residue was extracted into warm (30 ml) acetonitrile. Prolonged standing (2 days) at 0 °C afforded orange prisms of **4** (2.46 g, 52 %). Found: C, 76.41; H, 8.91; N, 3.01. C$_{130}$H$_{179}$ClNO$_8$Nb·3½MeCN requires C, 76.32; H, 8.86; N, 2.92 %. MS (positive nanospray in CH$_2$Cl$_2$/MeCN): 1937 (MH – Cl – MeCN), 1919 (M – Cl – MeCN – OH), 1902 (M – Cl – MeCN – 2OH), 1885 (M – Cl – MeCN – 3OH), (M – Cl – MeCN – 4OH). IR (Nujol, KBr, cm^{-1}): 3545w, 3523w, 3428w, 2295w, 2261w, 1651w, 1600w, 1391m, 1377m, 1323w, 1291m, 1260s, 1212s, 1190s, 1153w, 1121m, 1022m, 970w, 913m, 885s, 859m, 799s, 770w, 753w, 719m, 708w, 669w, 645w, 560w, 468w, 451w. ^{1}H NMR (C$_6$D$_6$): δ = 7.65 – 6.80 (6x m, 12H, aryl*H*), 5.45 (s, 2H, C*H*), 4.91 (s, 4H, O*H*), 2.18 (bs, 6H, *Me*CN), 1.51 (s, 36H, C(CH_3)$_3$), 1.23 (s, 36H, C(CH_3)$_3$).

Polymer Characterization

Polymerization Procedure

In toluene: Typical polymerization procedures in the presence of two equivalents of benzyl alcohol (Table 2, run 5) were as follows. A toluene solution of **1** (12.3 mmol, 1.0 mL toluene) and BnOH (0.012 mmol) were added into a Schlenk tube in the glove-box at room temperature. The solution was stirred for 2 min, and then ε-caprolactone (4.9 mmol) along with 1.5 mL toluene was added to the solution. The reaction mixture was then placed into an oil bath pre-heated at 110 °C, and the solution was stirred for the prescribed time (20 h). The polymerization mixture was then quenched by addition of an excess of glacial acetic acid (0.2 mL) into the solution, and the resultant solution was then poured into methanol (200 mL). The resultant polymer was then collected on filter paper and was dried *in vacuo*.

Without solvent: For example, to the metal complex **1** (0.383 g, 236.6 μmol) was added ε-caprolactone (5.19 ml, 47.3mmol) and where stated benzyl alcohol (0.01 ml, 118.3 μmol) and the system was placed in a pre-heated (100 °C) oil bath and stirred for 1 h. On cooling, the polymerization was quenched by pouring into excess (250 ml) heptane.

Crystallography.

Crystal data were collected on a Rigaku Saturn 724+ CCD diffractometer using synchrotron radiation at DLS beam line I19 for **L^1H_4**, using the same instrument but with sealed-tube MoKα radiation for **L^2H_4**·2MeCN, **1**·6MeCN, **2**·3½MeCN·0.614toluene, and **4**·3½MeCN, and a Stoe IPDS diffractometer for **3**·5MeCN and **4**·5MeCN. Data were corrected for Lp effects and for absorption, based on repeated and symmetry equivalent reflections and solved by direct methods or a dual-space method (SHELXS-2013/ SHELXT).[14, 15] Structures were refined by full matrix least squares on F^2.[16] H atoms were included in a riding model except for H(1), H(3) and H(4) in **L^2H_4**, and H(7) and H(8) in **4**·3½MeCN for which coordinates were refined. Hydrogen atom U_{iso} values were constrained to be 120 % of that of the carrier atom except for methyl and hydroxyl-H (150 %). Several structures exhibited two-fold disorder in, *tert*-butyl groups and/or solvent molecules where restraints were applied to geometry and anisotropic displacement parameters. For **4**·5MeCN, the crystal examined was a non-merohedral twin. The second twin component was identified on the diffractometer and both components integrated and used for refinement of the crystal structure. In this structure one MeCN of crystallization per unit cell was refined as a diffuse area of electron density by the Platon Squeeze procedure[17] and three MeCNs per asymmetric unit were refined at half weight. In **3**·5MeCN, four MeCNs per unit cell were refined using the Squeeze procedure.

Further details are provided in Tables 2a and 2b. CCDC 1043647-1043648 and 1043851-1043855 contain the supplementary crystallographic data for this paper. These data can be obtained free of charge from The Cambridge Crystallographic Data Centre via www.ccdc.cam.ac.uk/data_request/cif.

Acknowledgements

The EPSRC Mass Spectrometry Service (Swansea, UK) and the EPSRC National X-ray Crystallographic Service (Southampton) are thanked for data collection. Y. A-K thanks the higher committee for education development in Iraq for financial support.

Table 2a. Crystallographic data for the compounds L^1H_4, L^2H_4·2MeCN, **1**·6MeCN and **2**·3½MeCN·0.614toluene

Compound	**L^1H_4**	**L^2H_4**·2MeCN	**1**·6MeCN	**2**·3½MeCN·0.614toluene
Formula	$C_{64}H_{90}O_4$	$C_{64}H_{90}O_4\cdot 2(C_2H_3N)$	$C_{68}H_{92}Cl_6N_2Nb_2O_4\cdot 6(C_2H_3N)$	$C_{72}H_{102}Cl_4N_2O_6Nb_2\cdot 3½(C_2H_3N)\cdot 0.614(C_7H_8)$
Formula weight	923.35	1005.46	1646.27	1619.45
Crystal system	Triclinic	Triclinic	Triclinic	Triclinic
Space group	$P\bar{1}$	$P\bar{1}$	$P\bar{1}$	$P\bar{1}$
Unit cell dimensions				
a (Å)	11.778(11)	14.643(1)	10.8601(8)	12.6086(9)
b (Å)	15.190(15)	15.4125(11)	12.1510(9)	16.8197(12)
c (Å)	18.55(2)	16.1202(11)	17.9452(13)	21.7135(15)
α (°)	68.19(3)	75.412(12)	72.153(13)	89.714(2)
β (°)	83.42(5)	69.309(11)	79.492(15)	86.846(2)
γ (°)	69.19(4)	73.026(12)	77.185(14)	73.006(2)
V (Å^3)	2880(5)	3209.9(5)	2181.2(4)	4396.8(5)
Z	2	2	1	2
Temperature (K)	100(2)	100(2)	100(2)	100(2)
Wavelength (Å)	0.6889	0.71073	0.71073	0.71073
Calculated density (g.cm^{-3})	1.065	1.040	1.253	1.223
Absorption coefficient (mm^{-1})	0.06	0.06	0.50	0.43

Transmission factors (min./max.)	0.532 and 1.000	0.113 and 1.000	0.614 and 1.000	0.746 and 1.000
Crystal size (mm^3)	0.10 × 0.02 × 0.01	0.09 × 0.04 × 0.01	0.05 × 0.04 × 0.01	0.17 × 0.07 × 0.06
θ(max) (°)	22.5	22.5	25.0	27.6
Reflections measured	32266	21642	20034	77150
Unique reflections	8221	8056	7527	20127
R_{int}	0.179	0.216	0.094	0.051
Reflections with $F^2 > 2\sigma(F^2)$	4391	3030	4629	17091
Number of parameters	651	728	546	1054
R_1 [$F^2 > 2\sigma(F^2)$]	0.116	0.146	0.077	0.057
wR_2 (all data)	0.313	0.484	0.207	0.169
GOOF, S	1.10	1.03	1.05	1.02
Largest difference peak and hole (e Å^{-3})	0.34 and –0.27	1.17 and –0.32	1.36 and –0.96	1.22 and –1.68

Table 2b. Crystallographic data for the complexes **3**·3MeCN, **4**·3½MeCN and **4**·5MeCN

Compound	**3**·5MeCN	**4**·3½MeCN	**4**·5MeCN
Formula	$C_{72}H_{102}Cl_4N_2O_6Ta_2\cdot5(C_2H_3N)$	$C_{130}H_{179}ClNNbO_8\cdot3½(C_2H_3N)$	$C_{130}H_{179}ClNNbO_8\cdot5(C_2H_3N)$
Formula weight	1800.52	2155.78	2217.36
Crystal system	Triclinic	monoclinic	triclinic
Space group	$P\bar{1}$	$P2_1/c$	$P\bar{1}$
Unit cell dimensions			
a (Å)	12.6367(8)	30.358(2)	17.5553(17)
b (Å)	16.8848(11)	17.6674(12)	19.1574(15)
c (Å)	21.6085(14)	24.5131(17)	22.552(3)
α (º)	87.781(5)	90	74.926(8)
β (º)	87.412(5)	93.6385(17)	81.846(9)
γ (º)	73.944(5)	90	73.063(7)
V (Å^3)	4424.5(5)	13121.0(15)	6988.0(12)
Z	2	4	2
Temperature (K)	150(2)	100(2)	150(2)
Wavelength (Å)	0.71073	0.71073	0.71073
Calculated density (g.cm^{-3})	1.351	1.091	1.054
Absorption coefficient (mm^{-1})	2.64	0.17	0.16
Transmission factors (min./max.)	0.412 and 0.624	0.699 and 1.000	0.796 and 1.000
Crystal size (mm^3)	0.35 × 0.35 × 0.20	0.08 × 0.06 × 0.06	0.30 × 0.25 × 0.20
θ(max) (°)	25.5	25.0	19.8
Reflections measured	93502	69292	25016

Unique reflections	40462	22952	12529
R_{int}	0.039	0.072	0.138
Reflections with $F^2 > 2\sigma(F^2)$	26933	13966	3851
Number of parameters	862	1529	1396
R_1 $[F^2 > 2\sigma(F^2)]$	0.082	0.072	0.082
wR_2 (all data)	0.226	0.183	0.238
GOOF, S	0.94	1.06	0.79
Largest difference peak and hole (e Å^{-3})	2.48 and –2.77	0.89 and –0.90	0.50 and –0.30

References

[1] (a) M. Labet and W. Thielemans, *Chem. Soc. Rev.* 2009, **38**, 3484. (b) A. Arbaoui and C. Redshaw, *Polym. Chem.* 2010, **1**, 801. (c) X. Rong and C. Chunxia, *Prog. Chem.* 2012, **24**, 1519.

[2] Y. Kim, P.N. Kapoor and J.G. Verkade, *Inorg. Chem.* 2002, **41**, 4834.

[3] T.K. Saha, M. Mandel, M. Thunga, D. Chakraborty and V. Ramkumar, *Dalton Trans*. 2013, **42**, 10304.

[4] R. Galletti, G. Pampaloni, *Coord. Chem. Rev.* 2010, **254**, 525. (b) Y.R. Patil in: *Olefins Polymerisation Reactivity of Niobium-Based Metal Complexes*, US, Lambert Academic Publishing, 2011. (c) C. Redshaw, M. Walton, L. Clowes, D.L. Hughes, A.-M. Fuller, Y. Chao, A. Walton, V. Sumerin, P. Elo, I. Soshnikov, W. Zkao and W.-H. Sun, *Chem. Eur. J.* 2013, **19**, 8884.

[5] L.H. Tang, E.P. Wasserman, D.R. Neithamer, R.D. Krystosek, Y. Cheng, P.C. Price, Y.Y. He and T.J. Emge, *Macromolecules*, 2008, **41**, 7306.

[6] J. Zhang, C. Jian, Y. Gao, L. Wang, N. Tang and J. Wu, *Inorg. Chem*. 2012, **51**, 13380.

[7] A. Arbaoui, C. Redshaw and D.L. Hughes, *Chem. Commun*. 2008, 4717.

[8] (a) S. Singh and H. W. Roesky, *Dalton Trans.*, 2007, 1360. (b) M. Delferro, and T. J. Marks, *Chem. Rev*. 2011, **111**, 2450. (c) M. P. Weberski, Jr, C. Chen, M. Delferro, and T. J. Marks, *Chem. Eur. J.* 2012, **18,** 10715. (d) M. Delferro, and T. J. Marks, *Chem. Rev.* 2011, **111**, 2450–2485. (e) S. Liu, A. Motta, A.R. Mouat, M. Delferro, T.J. Marks, T.J. *J. Am. Chem. Soc*. 2014, *136*, 10460.

[9] See for example T.W. Coffindaffer, B.D. Steffy, I.P. Rothwell, K. Folting, J.C. Huffman and W.E. Streib, *J. Am. Chem. Soc*. 1989, **111**, 4749.

[10](a) H. Kawaguchi and T. Matsuo, *Inorg. Chem*. 2002, **41**, 6090. (b) C. Redshaw, D.M. Homden, M.A. Rowan and M.R.J. Elsegood, *Inorg. Chimica Acta*, 2005, **358**, 4067.

[11] G.R. Willey, T.J. Woodman and M.G.B. Drew, *Polyhedron*, 1997, **16**, 351.

[12] N. Ikpo, C. Hoffmann, L.N. Dawe and F.M. Kerton, *Dalton Trans*., 2012, **41**, 6651.

[13] V.C. Gibson, T.P. Kee and A. Shaw, *Polyhedron*, 1988, **7**, 2217.

[14] G.M. Sheldrick, *Acta Cryst*. 2008, **A64**, 112.

[15]G.M. Sheldrick, *Acta Cryst*., 2015, **A71**, 3.

[16]G.M. Sheldrick, *Acta Cryst*., 2015, **C71**, 3.

[17]A.L. Spek, *Acta Cryst*. 1990, **A46**, C34.

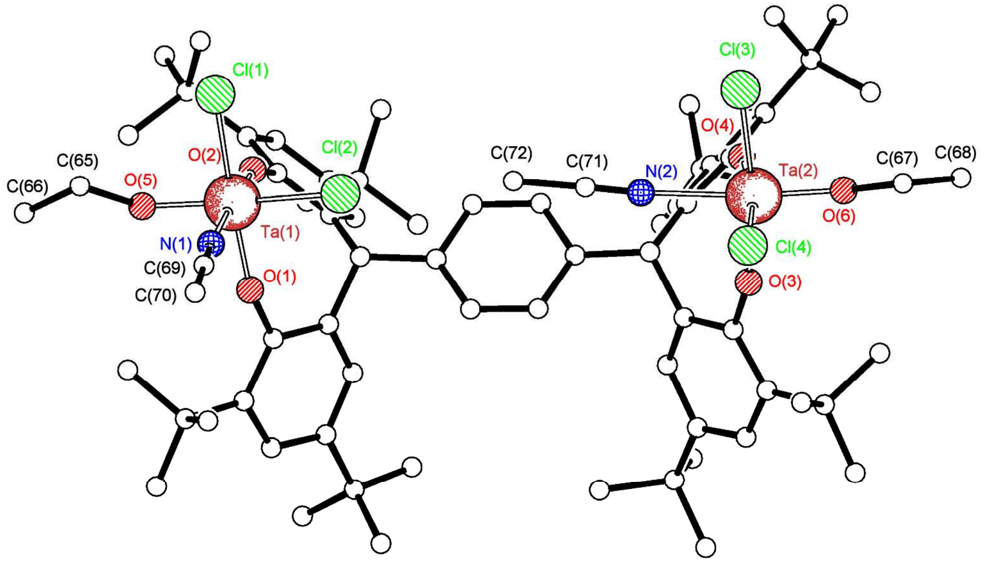
Cl(1)
Cl(3)
O(4)
O(2)
Cl(2)
C(65)
C(72)
C(71)
Ta(2)
C(67)
C(68)
C(66)
O(5)
N(2)
O(6)
Ta(1)
N(1)
Cl(4)
C(69)
O(1)
O(3)
C(70)